Available online at www.sciencedirect.com

ScienceDirect

Ceramics International 39 (2013) 9195–9199

CERAMICS INTERNATIONAL

www.elsevier.com/locate/ceramint

Sol–gel synthesis, characterization, and neurotoxicity effect of zinc oxide nanoparticles using *gum tragacanth*

Majid Darroudi[a,b,*], Zahra Sabouri[c], Reza Kazemi Oskuee[b,d], Ali Khorsand Zak[e], Hadi Kargar[c], Mohamad Hasnul Naim Abd Hamid[f]

[a]*Nuclear Medicine Research Center, School of Medicine, Mashhad University of Medical Sciences, Mashhad, Iran*
[b]*Department of Modern Sciences and Technologies, School of Medicine, Mashhad University of Medical Sciences, Mashhad, Iran*
[c]*Chemistry Department, Payame Noor University, 19395-4697 Tehran, Iran*
[d]*Targeted Drug Delivery Research Center, Mashhad University of Medical Sciences, Mashhad, Iran*
[e]*Electroceramics and Materials Laboratory, Physics Department, Faculty of Science, Ferdowsi University of Mashhad, Mashhad, Iran*
[f]*Center for Research & Instrumentation Management, Universiti Kebangsaan Malaysia, 43600 UKM Bangi, Selangor D. E., Malaysia*

Received 30 April 2013; accepted 5 May 2013
Available online 15 May 2013

Abstract

The use of plant extract in the synthesis of nanomaterials can be a cost effective and eco-friendly approach. In this work we report the "*green*" and biosynthesis of zinc oxide nanoparticles (ZnO-NPs) using *gum tragacanth*. Spherical ZnO-NPs were synthesized at different calcination temperatures. Transmission electron microscopy (TEM) imaging showed the formation most of nanoparticles in the size range of below 50 nm. The powder X-ray diffraction (PXRD) analysis revealed wurtzite hexagonal ZnO with preferential orientation in (101) reflection plane. *In vitro* cytotoxicity studies on neuro2A cells showed a dose dependent toxicity with non-toxic effect of concentration below 2 μg/mL. The synthesized ZnO-NPs using *gum tragacanth* were found to be comparable to those obtained from conventional reduction methods using hazardous polymers or surfactants and this method can be an excellent alternative for the synthesis of ZnO-NPs using biomaterials.

Keywords: A. Sol-gel processes; B. Electron microscopy; D. ZnO

1. Introduction

Zinc oxide (ZnO) is an inorganic semiconductor with a hexagonal wurtzite crystal structure which it has a wide and direct band gap (nearly 3.37 eV) at ambient temperature [1]. The ZnO-NPs has numerous applications such as catalysis [2], piezoelectric devices [3], pigment [4], chemical sensors [5], and cosmetic material especially for transparent UV protection [6]. It is important to prepare ZnO-NPs by a simple, cost effective, and eco-friendly process that has potential to yield nanoparticles of uniform particles in size. The various methods used for synthesis of these ZnO-NPs include solvothermal and hydrothermal synthesis [7–9], precipitation [10,11], polymerization method [12], laser ablation [13], sonochemical [14,15], and sol–gel [16–18] methods. The sol–gel method has gained much interest among researchers as it offers controlled consolidation, shape modulation, patterning of the nanostructures and low processing temperature [19,20].

Recently, biomaterials have been used to synthesize nanoparticles, particularly metal and metal oxide nanoparticles. *Citrus aurantifolia* extract [21], *Aloe vera* leaf extract [22], and milky latex of *Calotropis procera* [23] have been used in the synthesis of zinc oxide nanoparticles (ZnO-NPs). Polysaccharide hydrocolloids are high molecular weight macromolecules

*Corresponding author at: Nuclear Medicine Research Center, School of Medicine, Mashhad University of Medical Sciences, Mashhad, Iran. Tel.: +98 5118002286; fax: +98 511 8002287.
E-mail addresses: majiddarroudi@gmail.com, darroudim@mums.ac.ir (M. Darroudi).

0272-8842/$ - see front matter © 2013 Elsevier Ltd and Techna Group S.r.l. All rights reserved.
http://dx.doi.org/10.1016/j.ceramint.2013.05.021

such as alginate, agar–agar, starches, pectin, and gums. Gums are naturally occurring polysaccharide components in plants, which are mostly green, economical, and easily available [24].

Gum tragacanth (GT) is a naturally occurring complex, acidic polysaccharide derived as an exudate from the bark of *Astragalus gummifer* (Fabaceae family), a native tree of western Asia. It is commercially produced mostly in Iran and Turkey [25]. This biopolymer is an arabinogalactan type of natural gum and its structural, physicochemical, compositional, solution, thermal, rheological and emulsifying properties have been well characterized and studied [26,27]. This natural polymer consists of a mixture of water-soluble (tragacanthin) and water-swellable (bassorin) polysaccharide fractions [25,28].

In this study, we demonstrate a sol–gel method using GT to synthesize ZnO-NPs. Zinc nitrate was used as the zinc source at different calcination temperatures. The synthesized samples were then characterized using FESEM, TEM, XRD, TGA/DTA, and UV–vis spectroscopy. The majority of this research has investigated synthesis of nanoparticles in plants, proving that this method is eco-friendly, very cost effective, and can consequently be used as an economic and valuable alternative for the large-scale production of metal and metal oxide nanoparticles.

2. Materials and methods

2.1. Materials and reagents

The GT was obtained at a local health food store. The Zn $(NO_3)_2.6H_2O$ was of analytical grade and used as received without further purification.

2.2. Synthesis of ZnO-NPs

To prepare 1.5 g of ZnO-NPs, 4.5 g of $Zn(NO_3)_2.6H_2O$ was dissolved in 10 ml of distilled water and then stirred for 30 min. Meanwhile, 0.2 g of GT was dissolved in 40 ml of distilled water and stirred for 90 min at 60 °C to achieve a clear GT solution. After that, the zinc nitrate solution was added to the GT solution, and the container was moved to an oil bath. The temperature of the oil bath was fixed at 80 °C. Stirring was continued for 12 h to obtain a pale lemon color resin. The final product was calcined at different temperatures (400, 500, 600 and 700 °C) in air for 1 h to obtain ZnO-NPs.

2.3. Characterization of ZnO-NPs

The prepared ZnO-NPs were characterized by powder X-ray diffraction (PXRD, Philips, X'pert, Cu K_α), thermogravimetry analysis (TGA, Q600), UV–vis spectrophotometry (UV–vis, Evolution 300® Thermo Fisher Scientific), transmission electron microscopy (TEM, Hitachi H-7100), and field emission scanning electron microscopy (FESEM, Carl Zeiss Supra 55VP).

2.4. Evaluation of neurotoxicity effect

The cytotoxicity of nanoparticles was evaluated by a method using 3-(4,5-dimethylthiazol-2-yl)-2,5-diphenylte-trazolium bromide (MTT) assay [29]. Briefly, neuro2A cells were seeded at a density of 1×10^4 cells per well in 96-well plates and incubated for 24 h. Thereafter, the cells were treated with various concentrations of nanoparticles in the presence of 10% FBS. The calcined ZnO-NPs at 600 °C were suspended in a stock solution at 5 μg/ml in a solution of dimethyl sulfoxide (DMSO)/double distilled water. After 24 h of incubation, 20 μl of 5 mg/ml MTT in the PBS buffer was added to each well, and the cells were further incubated for 4 h at 37 °C. The medium containing unreacted dye was discarded, and 100 μl of DMSO was added to dissolve the formazan crystal formed by live cells. Optical absorbance was measured at 590 nm (reference wavelength 630 nm) using a microplate reader (Statfax-2100, Awareness Technology, USA), and cell viability was expressed as a percent relative to untreated control cells. Values of metabolic activity are presented as mean ± SD of triplicates.

3. Results and discussion

The thermogravimetric and derivative analysis (TGA/DTA) curves of the as-prepared gel by the sol–gel method in a GT environment are presented in Fig. 1. The heating process was started at 20 °C, and then increased up to 440 °C with a temperature rate change of 10 °C/min. The TGA curve descends until it becomes horizontal around 440 °C, and about 60% weight loss was observed during the heating process. The TGA/DTA traces show four main regions. The first weight loss between 20 and 140 °C (9%) is an initial loss of water, bend Ed1. The second weight loss from 140 °C to 220 °C (12.5%) is attributed to the decomposition of chemically bound groups, which corresponds to bend Ed2. The third step from 220 to 310 °C (31%) is related to both the decomposition of the organic groups, and the formation of the pyrochlore phases, bend Ed3. The last weight-loss step from 310 to 440 °C (7.5%) is attributed to the decomposition of the pyrochlore phases and

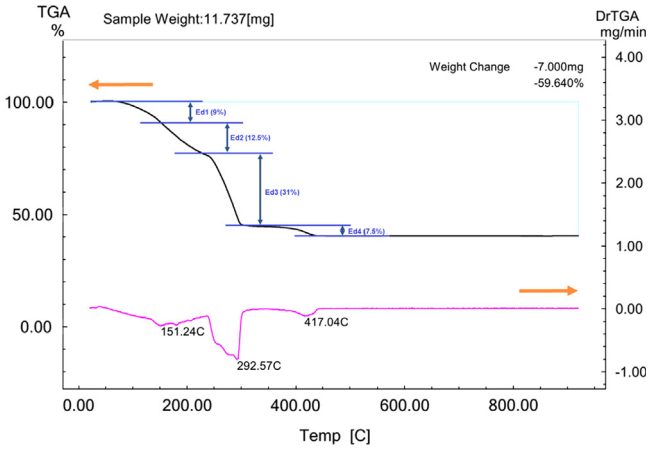

Fig. 1. TGA/DTA curves of gels from 20 °C to 920 °C. It shows about 60% weight loss in four steps to achieve ZnO-NPs.

the formation of ZnO pure phases indicated by bend Ed4. No weight loss between 440 and 920 °C was detected on the TGA curve, which indicates the formation of nanocrystalline ZnO as the decomposition product. Compare to our previous works, the pure phase is obtained at lower temperature [16,18].

The room temperature UV–vis absorption spectrum of the ZnO-NPs is shown in Fig. 2. The ZnO-NPs were dispersed in water with concentration of 0.1 wt% and then the solution was used to perform the UV–vis measurement. The spectrum reveals a characteristic absorption peak of ZnO at wavelength of 370 nm which can be assigned to the intrinsic band-gap absorption of ZnO due to the electron transitions from the valence band to the conduction band ($O_{2p} \rightarrow Zn_{3d}$) [18,30]. In addition, this sharp peak shows that the particles are in nano-size, and the particle size distribution is narrow. It is clearly shown that the maximum peak in the absorbance spectrum does not correspond to the true optical band gap of the ZnO-NPs. A common way to obtain the band gap from absorbance spectra is to get the first derivative of the absorbance with respect to photon energy and find the maximum in the derivative spectrum at the lower energy sides [31,32]. The derivative of the absorbance of the ZnO-NPs is shown in the inset of Fig. 2, and it indicates a band gap of 3.3 eV for the ZnO-NPs. The good absorption of the ZnO-NPs in the UV region proves the applicability of this product in such medical application such as sun-screen protectors or as antiseptic in ointments [33].

The PXRD patterns of the ZnO-NPs calcined at different temperatures of 400, 500, 600, and 700 °C are shown in Fig. 3a–d, correspondingly. All of the detectable peaks with the Miller indices (100), (002), (101), (102), (110), (103), (200), (112), (201), and (004) can be indexed to the ZnO wurtzite structure (JCPDS # 00-036-1451). The broadening of the peaks indicates that the crystalline size is in nanoscale [34] and this result indicates that the size of the obtained samples is fine and small (below 50 nm), as confirmed by the TEM image and its corresponding size distributions of prepared ZnO-NPs at 600 °C. After the as-prepared ZnO-NPs are calcined at different temperatures for 1 h, XRD peaks become sharper with increasing calcination temperatures and FWHM decreases, indicating that the crystallinity of ZnO-NPs is accelerated by the calcination process. Moreover, there were no other peaks related to an impurity for prepared ZnO-NPs at different calcination temperatures, indicating that the final nano powders were relatively pure.

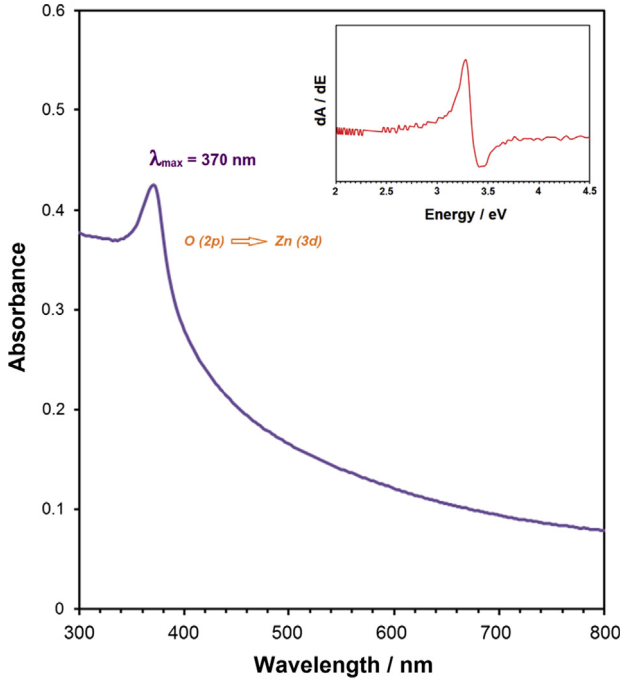

Fig. 2. UV–vis spectrum and band gap estimation (inset) of prepared ZnO-NPs at 600 °C.

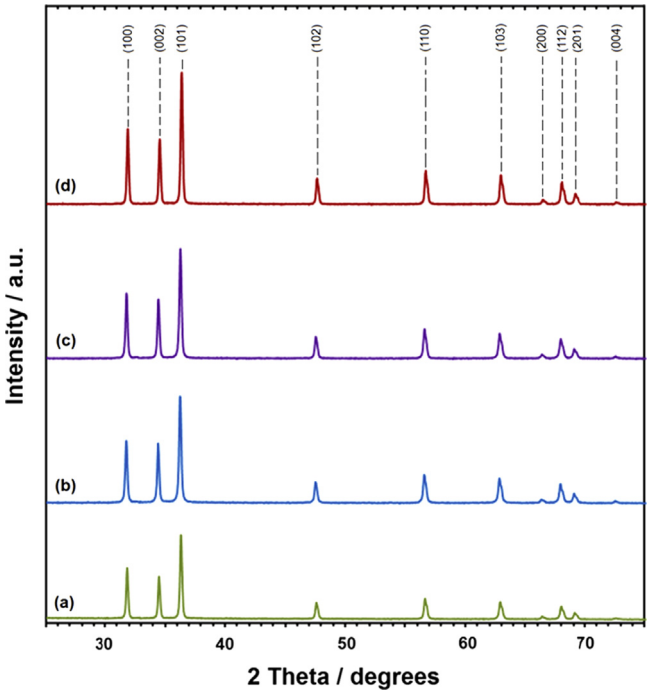

Fig. 3. PXRD patterns of synthesized ZnO-NPs in air at different temperatures (a: 400; b: 500; c: 600; and d: 700 °C).

The TEM and size distribution (Fig. 4) and FESEM (Fig. 5) confirm a narrow size distribution and high homogeneity of prepared ZnO-NPs which can be obtained in GT media.

The results of *in vitro* cytotoxicity studies after 24 h of incubation with different concentrations of nanoparticles, ranging from 0 to 100 μg/mL, are shown in Fig. 6. As the results showed, for concentration above 2 μg/mL the metabolic activity was decreased in a concentration dependent manner meaning that metabolic activity was started to decrease from 2 μg/mL and in 100 μg/mL maximal decreasing was observed.

4. Conclusion

ZnO-NPs were synthesized by the sol–gel method in *gum tragacanth* media. From XRD results, it was observed that all of the ZnO-NPs calcined at different temperatures exhibited the high purity with the hexagonal, wurtzite structure. The typical band gap was estimated from UV–vis spectrum and it was obtained to be about 3.3 for the sample calcined at 600 °C.

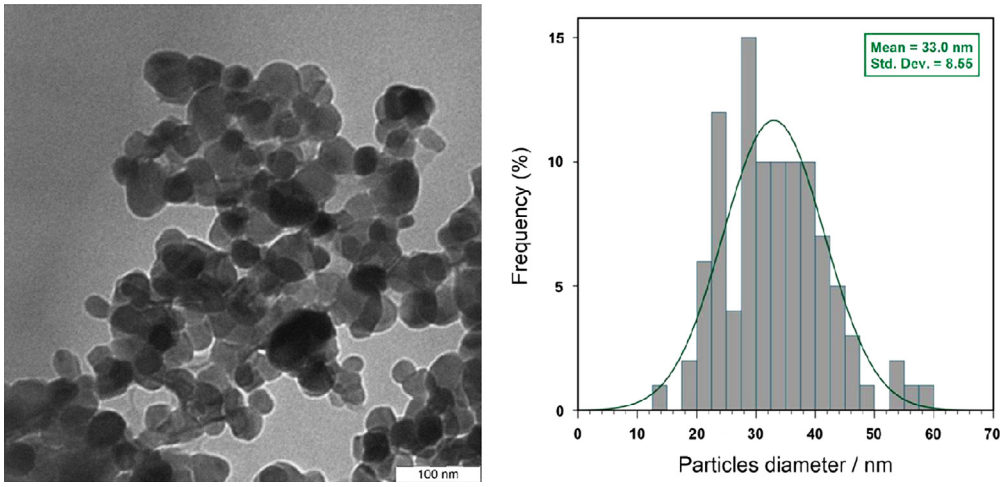

Fig. 4. TEM image and corresponding size distribution of prepared ZnO-NPs at 600 °C.

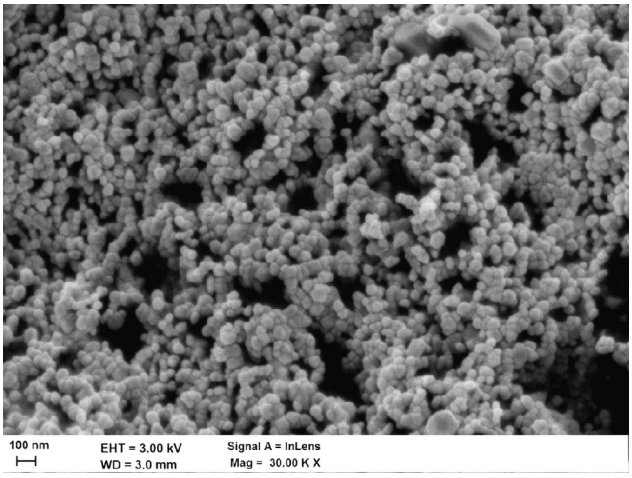

Fig. 5. FESEM image of prepared ZnO-NPs at 600 °C.

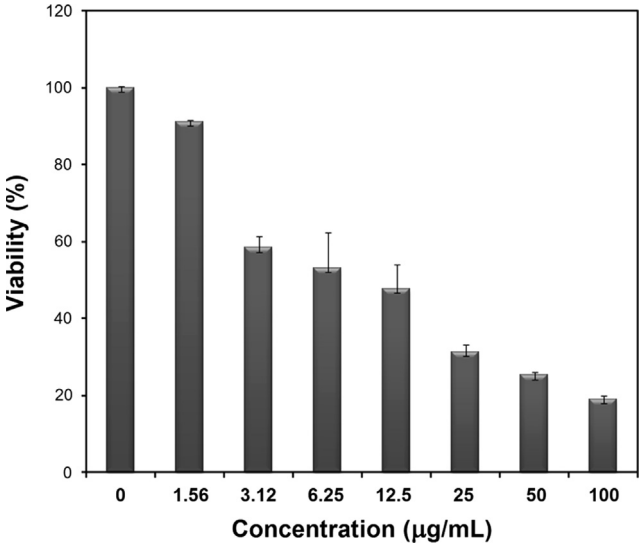

Fig. 6. Cell viability of neuro2A cells measured by the MTT assay. Cells were incubated for 24 h with the indicated concentrations of the nanoparticles.

This method is interesting for applying and extending the green chemistry rules in preparation of nanoparticles. The other advantages of the method are simple synthesis, in a normal atmosphere, and low cost, giving a potential avenue for further practical scale-up of the production process and applications. It is expected that these nanoparticles can find potential applications in different fields such as cosmetics and optical/electrical devices as well as medicinal applications.

References

[1] Z.L. Wang, ZnO nanowire and nanobelt platform for nanotechnology, Materials Science & Engineering R—Reports 64 (2009) 33–71.
[2] W.F. Elseviers, H. Verelst, Transition metal oxides for hot gas desulphurization, Fuel 78 (1999) 601–612.
[3] S. Fujihara, H. Naito, T. Kimura, Visible photoluminescence of ZnO nanoparticles dispersed in highly transparent MgF_2 thin-films via sol–gel process, Thin Solid Films 389 (2001) 227–232.
[4] F.A. Sigoli, M.R. Davolos, M. Jafelicci, Morphological evolution of zinc oxide originating from zinc hydroxide carbonate, Journal of Alloys and Compounds 262 (1997) 292–295.
[5] R. Mochinaga, T. Yamasaki, T. Arakawa, The gas sensing of $SmCoO_x$/MO_x (M = Fe, Zn, In, Sn) having a heterojunction, Sensors and Actuators B—Chemical 52 (1998) 96–99.
[6] H. Akiyama, O. Yamasaki, H. Kanzaki, J. Tadaa, J. Arata, Effects of zinc oxide on the attachment of *Staphylococcus aureus* strains, Journal of Dermatological Science 17 (1998) 67–74.
[7] R. Razali, A.K. Zak, W.H.A. Majid, M. Darroudi, Solvothermal synthesis of microsphere ZnO nanostructures in DEA media, Ceramics International 37 (8) (2011) 3657–3663.
[8] Q. Li, Z. Kang, B. Mao, E. Wang, C. Wang, C. Tian, S. Li, One-step polyoxometalate-assisted solvothermal synthesis of ZnO microspheres and their photoluminescence properties, Materials Letters 62 (2008) 2531–2534.
[9] H.Y. Xu, H. Wang, Y.C. Zhang, W.L. He, M.K. Zhu, B. Wang, H. Yan, Hydrothermal synthesis of zinc oxide powders with controllable morphology, Ceramics International 30 (2004) 93–97.
[10] C.L. Kuo, C.L. Wang, H.H. Ko, W.S. Hwang, K.M. Chang, W.L. Li, H.H. Huang, Y.H. Chang, M.C. Wang, Synthesis of zinc oxide nanocrystalline powders for cosmetic applications, Ceramics International 36 (2010) 693–698.

[11] R. Song, Y. Liu, L. He, Synthesis and characterization of mercaptoacetic acid modified ZnO nanoparticles, Solid State Science 10 (2008) 1563–1567.
[12] P. Jajarmi, Fabrication of pure ZnO nanoparticles by polymerization method, Materials Letters 63 (2009) 2646–2648.
[13] R. Zamiri, A. Zakaria, H.A. Ahangar, M. Darroudi, A.K. Zak, G.P.C. Drummen, Aqueous starch as a stabilizer in zinc oxide nanoparticle synthesis via laser ablation, Journal of Alloys and Compounds 516 (2012) 41–48.
[14] C. Deng, H. Hu, G. Shao, C. Han, Facile template-free sonochemical fabrication of hollow ZnO spherical structures, Materials Letters 64 (2010) 852–855.
[15] A. Khorsand Zak, W.H.A. Majid, H.Z. Wang, Ramin Yousefi, A. Moradi Golsheikh, Z.F. Ren, Sonochemical synthesis of hierarchical ZnO nanostructures, Ultrasonics Sonochemistry 20 (2013) 395–400.
[16] A.K. Zak, W.H.A. Majid, M. Darroudi, R. Yousefi, Synthesis and characterization of ZnO nanoparticles prepared in gelatin media, Materials Letters 65 (2011) 70–73.
[17] F. Bigdeli, A. Morsali, Synthesis ZnO nanoparticles from a new Zinc(II) coordination polymer precursor, Materials Letters 64 (2010) 4–5.
[18] A. Khorsand Zak, W.H. Abd. Majid, M.R. Mahmoudian, Majid Darroudi, Ramin Yousefi Starch-stabilized synthesis of ZnO nanopowders at low temperature and optical properties study, Advanced Powder Technology 24 (2013) 618–624.
[19] B. Sunandan, D. Joydeep, Hydrothermal growth of ZnO nanostructures, Science and Technology of Advanced Materials 10 (2009) 013001.
[20] E.G. Lori, D.Y. Benjamin, L. Matt, Z. David, Y. Peidong, Solution grown zinc oxide nanowires, Inorganic Chemistry 45 (2006) 7535–7543.
[21] N.A. Samat, R.M. Nor, Sol–gel synthesis of zinc oxide nanoparticles using *Citrus aurantifolia* extracts, Ceramics International 39 (2013) S545–S548.
[22] G. Sangeetha, S. Rajeshwari, R. Venckatesh, Green synthesis of zinc oxide nanoparticles by *Aloe barbadensis* miller leaf extract: structure and optical properties, Materials Research Bulletin 46 (2011) 2560–2566.
[23] R.P. Singh, V.K. Shukla, R.S. Yadav, P.K. Sharma, P.K. Singh, A.C. Pandey, Biological approach of zinc oxide nanoparticles formation and its characterization, Advanced Materials Letters 2 (2011) 313–317.
[24] V. Rana, P. Rai, A.K. Tiwary, R.S. Singh, J.F. Kennedy, C.J. Knill, Modified gums: approaches and applications in drug delivery, Carbohydrate Polymers 83 (2011) 1031–1047.
[25] G.O. Phillips, P.A. Williams, Handbook of Hydrocolloids, Woodhead Publishing Limited, Cambridge, 2009.
[26] M.J. Zohuriaan, F. Shokrolahi, Thermal studies on natural and modified gums, Polymer Testing 23 (2004) 575–579.
[27] F. Chenlo, R. Moreira, C. Silva, Rheological behavior of aqueous systems of tragacanth and guar gums with storage time, Journal of Food Engineering 96 (2010) 107–113.
[28] N. Gralen, M. Karrholm, The physicochemical properties of solutions of gum tragacanth, Journal of Colloid Science 5 (1950) 21–36.
[29] T. Mosmann, Rapid colorimetric assay for cellular growth and survival: application to proliferation and cytotoxicity assays, Journal of Immunological Methods 65 (1983) 55–63.
[30] A. Khorsand Zak, R. Yousefi, W.H.A. Majid, M.R. Muhamad, Facile synthesis and X-ray peak broadening studies of $Zn_{1-x}Mg_xO$ nanoparticles, Ceramics International 38 (2012) 2059–2064.
[31] A. Khorsand Zak, R. Razali, W.H.A. Majid, M. Darroudi, Synthesis and characterization of a narrow size distribution of zinc oxide nanoparticles, International Journal of Nanomedicine 6 (2011) 1399–1403.
[32] M. Darroudi, M. Hakimi, M. Sarani, R. Kazemi Oskuee, A. Khorsand Zak, L. Gholami, Facile synthesis, characterization, and evaluation of neurotoxicity effect of cerium oxide nanoparticles, Ceramics International 39 (2013) 6917–6921.
[33] F. Harding, Breast Cancer: Cause–Prevention–Cure, Aylesbury, Tekline Publishing, 2006.
[34] B. Djuricic, S. Pickering, Nanostructured cerium oxide: preparation and properties of weakly-agglomerated powders, Journal of the European Ceramic Society 19 (1999) 1925–1934.